

# Comparative study of the frequency-doubling performance on ring and linear cavity at short wavelength region

Wenhai Yang, Yajun Wang, Yaohui Zheng,\* and Huadong Lu

State Key Laboratory of Quantum Optics and Quantum Optics Devices, Institute of Opto-Electronics, Shanxi University, Taiyuan 030006, China

\*[yhzheng@sxu.edu.cn](mailto:yhzheng@sxu.edu.cn)

**Abstract:** We theoretically and experimentally perform a comparative study on performance of the linear standing-wave cavity and ring cavity for external cavity frequency doubling at the wavelength from 795 nm to 397.5 nm. The two cavities show obvious differences of the thermal effect of nonlinear crystal, cavity sensitivity, and maximum output power. The results show that ring cavity as the external enhancement cavity is a better choice than standing-wave cavity at short wavelength region. At last, a 397.5 nm violet laser with 408 mW corresponding to an input power of 992 mW is obtained by using the ring cavity, considering the original mode-matching efficiency of 98% between the 795 nm laser and frequency doubling cavity, the conversion efficiency is 41.9%.

© 2015 Optical Society of America

**OCIS codes:** (140.3515) Lasers, frequency doubled; (140.4780) Optical resonators; (190.2620) Harmonic generation and mixing; (190.4870) Photothermal effects.

---

## References and links

1. P. Grangier, R. E. Slusher, B. Yurke, and A. Laporta, "Squeezed-light-enhanced polarization interferometer," *Phys. Rev. Lett.* **59**(19), 2153–2156 (1987).
2. J. L. Sørensen, J. Hald, and E. S. Polzik, "Quantum noise of an atomic spin polarization measurement," *Phys. Rev. Lett.* **80**(16), 3487–3490 (1998).
3. Z. X. Xu, Y. L. Wu, L. Tian, L. R. Chen, Z. Y. Zhang, Z. H. Yan, S. J. Li, H. Wang, C. D. Xie, and K. C. Peng, "Long lifetime and high-fidelity quantum memory of photonic polarization qubit by lifting zeeman degeneracy," *Phys. Rev. Lett.* **111**(24), 240503 (2013).
4. G. Hetet, O. Glockl, K. A. Pilypas, C. C. Harb, B. C. Buchler, H. A. Bachor, and P. K. Lam, "Squeezed light for bandwidth-limited atom optics experiments at the rubidium D1 line," *J. Phys. B: At. Mol. Opt. Phys.* **40**, 221–226 (2007).
5. T. Tanimura, D. Akamatsu, and Y. Yokoi, A. Furusawa, M. Kozuma, "Generation of a squeezed vacuum resonant on a rubidium D1 line with periodically poled KTiOPO<sub>4</sub>," *Opt. Lett.* **31**(15), 2344–2346 (2006).
6. A. Predojevic, Z. Zhai, J. M. Caballero, and M. W. Mitchell, "Rubidium resonant squeezed light from a diode-pumped optical-parametric oscillator," *Phys. Rev. A* **78**, 063820 (2008).
7. H. Vahlbruch, M. Mehmet, S. Chelkowski, B. Hage, A. Franzen, N. Latstzka, S. Gossler, K. Danzmann, and R. Schnabel, "Observation of squeezed light with 10 dB quantum-noise reduction," *Phys. Rev. Lett.* **100**(3), 033602 (2008).
8. M. Mehmet, S. Ast, T. Eberle, S. Steinlechner, H. Vahlbruch, and R. Schnabel, "Squeezed light at 1550 nm with a quantum noise reduction of 12.3 dB," *Opt. Express* **19**(25), 25763–25772 (2011).
9. X. Wen, Y. S. Han, J. D. Bai, J. He, Y. H. Wang, B. D. Yang, and J. M. Wang, "Cavity-enhanced frequency doubling from 795 nm to 397.5 nm ultra-violet coherent radiation with PPKTP crystals in the low pump power regime," *Opt. Express* **22**(26), 32293–32300 (2014).

10. Y. S. Han, X. Wen, J. D. Bai, B. D. Yang, Y. H. Wang, J. He, and J. M. Wang, "Generation of 130 mW of 397.5 nm tunable laser via ring-cavity-enhanced frequency doubling," *J. Opt. Soc. Am. B* **31**(8), 1942–1947 (2014).
11. Y. H. Cha, K. H. Ko, G. Lim, J. M. Han, H. M. Park, T. S. Kim, and D. Y. Jeong, "External-cavity frequency doubling of a 5-W 756-nm injection-locked Ti:sapphire laser," *Opt. Express* **16**(7), 4866–4871 (2008).
12. M. Pizzocaro, D. Calonico, P. C. Pastor, J. Catani, G. A. Costanzo, F. Levi, and L. Lorini, "Efficient frequency doubling at 399 nm," *Appl. Opt.* **53**(16), 3388–3392 (2014).
13. F. Billa, A. Chiummo, E. Giacobino, and A. Bramati, "High-efficiency blue-light generation with a ring cavity with periodically poled KTP," *J. Opt. Soc. Am. B* **24**(3), 576–580 (2007).
14. M. Moller, L. M. Hoffer, G. L. Lippi, T. Ackemann, A. Gahl, and W. Lange, "Fabry-Perot and ring cavity configurations and transverse optical patterns," *J. Mod. Opt.* **45**(9), 1913–1926 (1998).
15. Y. H. Zheng, F. Q. Li, Y. J. Wang, K. S. Zhang, and K. C. Peng, "High-stability single-frequency green laser with a wedge Nd:YVO<sub>4</sub> as a polarizing beam splitter," *Opt. Commun.* **283**, 309 (2010).
16. S. Burks, J. Ortalo, A. Chiummo, X. Jia, F. Villa, A. Bramati, J. Laurat, and E. Giacobino, "Vacuum squeezed light for atomic memories at the D2 cesium line," *Opt. Express* **17**(5) 3777–3781 (2009).
17. K. Hayasaka, Y. Zhang, and K. Kasai, "Generation of 22.8 mW single-frequency green light by frequency doubling of a 50-mW diode laser," *Opt. Express* **12**(15), 3567–3572 (2004).
18. W. R. Bosenberg, A. Drobshoff, and J. I. Alexander, "93% pump depletion, 3.5-W continuous-wave, singly resonant optical parametric oscillator," *Opt. Lett.* **21**(17), 1336–1338 (1996).
19. H. D. Lu, X. J. Sun, M. H. Wang, J. Su, and K. C. Peng, "Single-frequency Ti:sapphire laser with continuous frequency-tuning and low intensity noise by means of the additional intracavity nonlinear loss," *Opt. Express* **22**(20), 24551–24558 (2014).
20. R. W. P. Drever, J. L. Hall, F. V. Kowalski, J. Hough, G. M. Ford, A. J. Munley, and H. Ward, "Laser phase and frequency stabilization using an optical resonant," *Appl. Phys. B* **31**, 97–105 (1983).
21. K. Durak, C. H. Nguyen, V. Leong, S. Straupe, and C. Kurtzseifer, "Diffraction-limited Fabry-Perot cavity in the near concentric regime," *New J. Phys.* **16**, 103002 (2014).
22. J. A. Zheng, S. Z. Zhao, Q. P. Wang, X. Y. Zhang, and L. Chen, "Influence of thermal effect on KTP type-II phase-matching second-harmonic generation," *Opt. Commun.* **199**, 207–214 (2001).
23. M. Sabaeian, L. Mousave, and H. Nadgaran, "Investigation of thermally-induced phase mismatching in continuous-wave second harmonic generation: A theoretical model," *Opt. Express* **18**(18), 18732 (2010).
24. M. E. Innocenzi, H. T. Yura, C. L. Fincher, and R. A. Fields, "Thermal modeling of continuous-wave end-pumped solid-state lasers," *Appl. Phys. Lett.* **56**(19) 1831–1833 (1990).
25. N. Uehara, E. K. Gustafson, M. M. Fejer, and R. L. Byer, "Modeling of efficient mode matching and thermal-lensing effect on a laser-beam coupling into a mode-cleaner cavity," *Proc. SPIE* **2989**, 57–68 (1997).
26. Yajun Wang, Wenhai Yang, Haijun Zhou, Meiru Huo, and Yaohui Zheng, "Temperature dependence of the fractional thermal load of Nd:YVO<sub>4</sub> at 1064 nm lasing and its influence on laser performance," *Opt. Express* **21**(15), 18068 (2013).
27. R. L. Targat, J.-J. Zondy, and P. Lemonde, "75%-Efficiency blue generation from an intracavity PPKTP frequency doubler," *Opt. Commun.* **247**, 471–481 (2005).

---

## 1. Introduction

Generating the squeezed state resonant on the atomic transition line is a critical task not only for quantum information but also for ultraprecise measurement of atomic spins [1, 2]. Many of these quantum optics experiments are performed by using transitions at the Rubidium D1 line at 795 nm [3]. The generation of squeezing at this wavelength has therefore been the subject of many experimental efforts [4–6]. The optical parametric down-conversion process is the most effective method of generating the squeezed state [7, 8]. However, the process needs the second harmonic of 795 nm (397.5 nm light) as the pump source. So preparation of 397.5 nm lasing is an important premise for the squeezed state generation at 795 nm.

External cavity frequency doubling is an effective method of generating the violet wavelength laser source [9–12]. However, the wavelength of 397.5 nm is at the cut-off wavelength of many non-linear optical crystals (i.e the most popular crystal, periodically poled potassium titanyl phosphate PPKTP) along with high absorption coefficient, which induces severe thermal effect and grey tracking, when it is used for second-harmonic generator (SHG) at higher power density level [9, 13]. So it faces the challenge of obtaining enough output power. Due to its low absorption at 397.5 nm and no grey tracking effect, Lithium triborate (LBO) crystal, is suitable for SHG at high power level [12]. However, its temperature of non-critical phase-

matching is about 663 °C, which is hard to operate stably. For critical phase-matching, large walk-off angle makes the beam quality of second harmonic wave worse, only 76% of mode-matching efficiency for optical parameter oscillator (OPO) is obtained with this crystal as a doubler (while it is 98% for PPKTP doubler), which is difficult to obtain good mode matching for the application of squeezed state generation.

So reducing the thermal effect of the PPKTP crystal as far as possible is the key process to obtain the satisfying output power and beam quality. For a given nonlinear crystal and interaction wavelength, cavity configuration is another important determinant of the thermal effect. The simplest configuration for external enhancement cavity is the linear standing-wave cavity (SWC), which has the merit of low round trip loss. However, in this case, second-harmonic light is generated in both directions of propagation. The forward- and the backward-generated harmonic waves (and fundamental waves) do not only form the standing-wave in the linear cavity but also increase the absorption loss induced from the double pass [14]. For low absorption wavelength, the influence of the standing-wave and the double pass on the absorption can be neglected. For high-absorption wavelength, especially 397.5 nm, the double-pass absorption can result in serious thermal effect. Another common resonant cavity is the ring cavity (RC), which is usually a bow-tie-type configuration with two spherical mirrors and two flat mirrors [4, 5, 15–17]. The beams (including the fundamental wave and harmonic wave) travel only in one of the two possible directions, which is no standing-wave pattern and double-pass absorption in the nonlinear crystal. The shortcoming of the RC is more linear loss and poorer stability than the SWC. Walter et al have demonstrated the difference of spectral properties between SWC and RC, which is used as OPO [18]. Many authors obtained the 397.5 nm laser output by external cavity frequency doubling by using linear SWC or RC. However none of them presented a detailed study about the performance comparison (including thermal effect of nonlinear crystal, cavity sensitivity, and maximum output power) between the SWC and the RC.

In our experiment, we use a home-made single-frequency Ti:Sapphire laser tuned to 795 nm to pump a second-harmonic generator, and obtain the laser output of 397.5 nm. A SWC and RC are used as the second-harmonic generator, respectively. By comparing the thermal effect of the nonlinear crystal, resonant cavity sensitivity, and maximum output power of the two cavities, we find that RC is a better choice than SWC to obtain a high power and good beam quality SHG beam at the short wavelength region. A 397.5 nm violet laser of 408 mW with an input power of 992 mW is obtained by using the RC, considering the mode-matching efficiency of 98% between the 795 nm laser and frequency doubling cavity, the conversion efficiency is 41.9%.

## 2. Experimental setup

A home-made continuous-wave Ti:sapphire laser is employed in this experiment, with the maximum output power of 1.27 W, which is tuned to 795 nm resonant on Rubidium D1 line (720 nm–820 nm) [19]. The beam from the Ti:sapphire laser was phase modulated by an electro-optic modulator (EOM). This modulation is utilized to lock a cavity for frequency doubling by using the Pound-Drever-Hall (PDH) method [20].

We characterized the two external resonator configurations (SWC and RC) as shown in Fig. 1. Both configurations are designed with the same size of mode waist and PPKTP crystal. The PPKTP is 10 mm long with a cross section of 1×2 mm, and located at the waist position of the two curved mirrors. The crystal has a poling period of 3.15 μm for quasi-phase matching. The two end faces of the crystal have antireflection coatings with power reflectivities of 0.2% and 0.5% at each surface at the fundamental and harmonic wave. The crystal is placed in an oven and operated around the temperature of 55 °C to obtain the optimal phase-matching. The operating temperature of the oven ranges from 14 °C to 75 °C, corresponding to optimal

output wavelength range of 396.45 nm–398.14 nm. One of the external cavities (SWC) in Fig. 1 consists of two curved mirrors. The two curved mirrors have curvature radius of 30 mm and are separated by 62 mm. The input coupler has reflectivities of 85% and 99% at the fundamental and harmonic waves, which has crescent-shaped configuration to eliminate aberrations in the optical mode [21]. The output coupler has reflectivities of 99.5% and 1% at the fundamental and harmonic waves. The round trip loss of the fundamental wave is 3.6% for the SWC, including the PPKTP absorption loss of the double pass.

Another external cavity (RC) in Fig. 1 is a bow-tie-type ring configuration with two spherical mirrors (radius of curvature of 100 mm) and two flat mirrors. The input coupler is a flat mirror with a reflectivity of 85% at the fundamental wave, while the others are high-reflectivity coated for the fundamental wave. The spacing between the two spherical mirrors is 127.5 mm, and the total cavity length is 560 mm. For the RC, the fundamental wave passes the PPKTP crystal only once, the round trip loss for the fundamental wave is also 3.6%. And both of the two cavities are locked via the PDH technique with the modulation frequency of 72 MHz. The error signal is read from transmitted signal of the SHG, then feedback to a piezoelectric ceramics adhered to one of the cavity mirrors.

For the SHG at 795 nm wavelength, due to the high absorption coefficient at 397.5 nm, the thermal effect of the nonlinear crystal induced from the absorption can not be neglected. So it will be of the utmost importance to compare the discrepancy induced from the difference of the fractional thermal load between the SWC and the RC. In order to compare conveniently the discrepancy of the thermal effects, the two cavities are carefully adjusted to have identical mode size located at the PPKTP crystal, which ensures the difference of fraction thermal load is only caused by the type of the cavity.

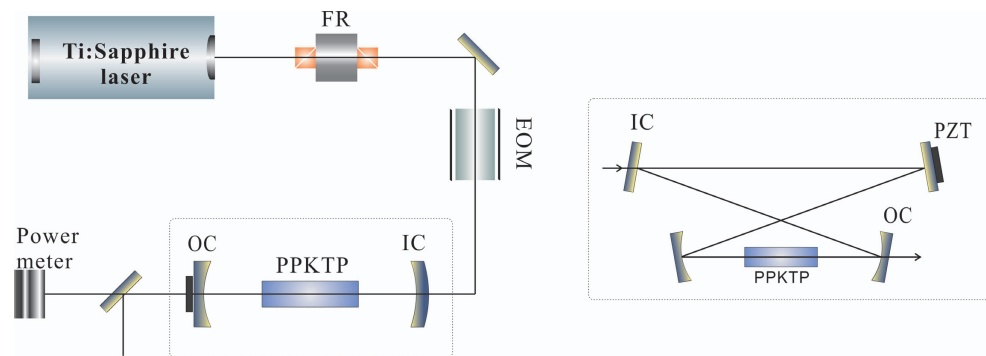


Fig. 1. Schematic of the experimental setup. The doubler is formed by linear standing-wave cavity and ring cavity, respectively. FR: Faraday rotator; EOM: electro-optical modulator.

### 3. Comparison of thermal effect

High absorption of 397.5 nm wavelength light generates the temperature gradient in the PPKTP crystal. This will lead to a nonuniform distribution of temperature as well as refractive index [22], thus perfect phase matching condition of SHG could not be maintained across intersecting surface of the beam, resulting in a limited SHG efficiency [23]. So it is of the utmost importance to compare the thermal effect induced from the absorption of the harmonic wave in the SWC with that in the RC.

Comparing with the RC, the SWC has a longitudinal interference between the two counterpropagating waves, which have an additional influence on the interaction with a nonlinear medium in the resonator. In our system, in order to simplify the analysis process, the longi-

tudinal interference effect is neglected. Thus the SWC can be unfolded into equivalent linear traveling wave cavity, the first half of its round trip in the traveling wave cavity corresponds to the forward half of the round trip in the SWC, and the second half of its round trip in the traveling wave cavity corresponds to the backward half of the round trip in the SWC [14]. Ignoring the effects of astigmatism, it is easy to see that the unfolding transformations of the linear SWC illustrated in Fig. 2 create a ring cavity with all the properties of the original SWC. The PPKTP crystal appears twice, representing the two encounters in the forward and the backward propagation. For the RC, The fundamental- and harmonic-waves propagate through the PPKTP crystal only once in every round trip.

To obtain the absorption information of the PPKTP crystal at the wavelengths of 795 nm and 397.5 nm, we perform an experiment of the single pass test, in which the incident beams are aligned with the same parameters as the mode size in the two cavities. With the experiment results, we found that the absorption at 795 nm is less than  $0.001 \text{ cm}^{-1}$ , which can be neglected for the input power of watt-level. The absorption at 398 nm is  $0.186 \text{ cm}^{-1}$ , which brings seriously thermal load in PPKTP. So we only consider the absorption for 397.5 nm.

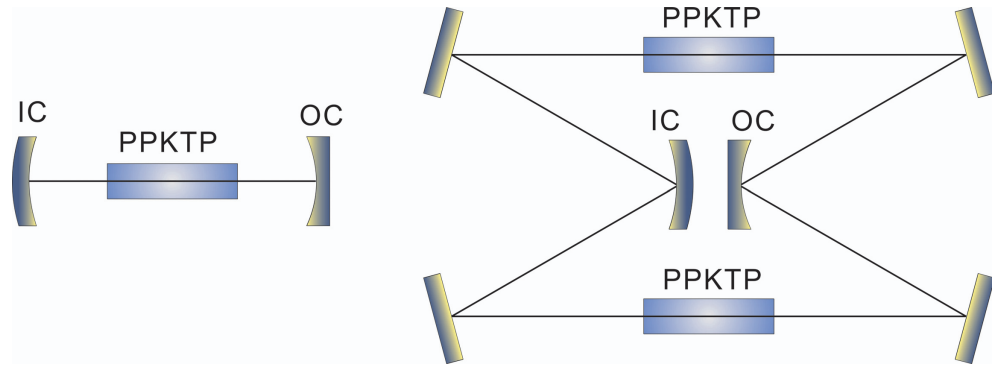


Fig. 2. Unfolding transformation of the linear standing-wave cavity. IC: input coupler; OC: output coupler. The PPKTP crystal appears twice in every round trip.

Under the plane-wave approximation, ignoring the thermal effect, the second-harmonic power from the external cavity frequency doubling can be expressed by [22]:

$$P_{2\omega} = \frac{8\omega^2 d_{eff}^2 l^2}{c^3 \epsilon_0 (n_e^2 \omega) (n_e^\omega)^2} \frac{P_{cir}^2}{4\pi \omega_0^2} \quad (1)$$

Where,  $\omega$  is the angle frequency of fundamental wave,  $d_{eff}$  is the effective nonlinear coefficient,  $c$  is the light velocity in vacuum,  $\epsilon_0$  is the vacuum dielectric constant,  $n$  is the refraction index,  $\omega_0$  is the beam radius of fundamental wave at the location of the PPKTP considered as a constant,  $P_{cir}$  is the circulating power of fundamental wave.  $P_{cir}$  is equal to the input power  $P_{in}$  enhanced by a factor, which is determined by the input mirror transmittance  $T$ , intracavity loss  $L$  and nonlinear loss  $\Gamma$  of the external cavity. It is

$$P_{cir} = P_{in} \frac{T}{\left(1 - \sqrt{(1-T)}\sqrt{(1-L)}\sqrt{(1-\Gamma(P_{cir}))}\right)^2} \quad (2)$$

For the same generating power, the light beam propagates through the PPKTP crystal two times every round trip for the SWC, while only once for the RC. Therefore, for the RC, the absorption efficiency  $\eta$  of PPKTP with length  $l$  and absorption coefficient  $\alpha$  can be expressed

by:

$$\eta_{RC} = 1 - e^{-\alpha l} \quad (3)$$

For the SWC, the absorption efficiency  $\eta$  of PPKTP with length  $l$  and absorption coefficient  $\alpha$  can be expressed by:

$$\eta_{SWC} = 1 - e^{-2\alpha l} \quad (4)$$

The temperature gradient results in refractive index gradient of the PPKTP crystal. The refractive index gradient associated with thermal focus length can be expressed as [24]

$$f = \frac{\pi K_c \omega_0^2}{\eta P_{2\omega} (dn/dT)} \quad (5)$$

Where,  $K_c$  is the thermal conductivity,  $dn/dT$  is the thermo-optic coefficient. Employing Eqs. (1)-(5) with the parameters  $K_c = 0.13$  W/cm/K,  $dn/dT = 22 \times 10^{-6}/^\circ\text{C}$ ,  $d_{eff} = 2d_{33}/\pi = 10.8$  pm/V ( $d_{33} = 16.9$  pm/V),  $\epsilon_0 = 8.85 \times 10^{-12}$  F/m,  $n_e^\omega = 1.844$  and  $n_e^{2\omega} = 1.968$ , the relationship between the thermal focus length  $f$  and input fundamental power for SWC and RC are shown in Fig. 3. For the same variation of input power, the thermal focus length located in the SWC changes from  $\infty$  to 30 mm, while the thermal focus length located in the RC changes only from  $\infty$  to 55 mm. It is obvious that the thermal effect of PPKTP located in the SWC is more severe than that located in the RC.

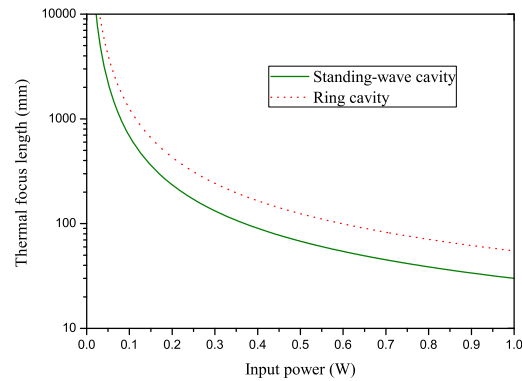


Fig. 3. Thermal focus length as a function of the input power. Real line: standing-wave cavity; Dashed line: ring cavity.

#### 4. Comparison of resonator sensitivity

Resonators with thermal lens suffer from several disadvantages which make them unacceptable for external resonator frequency doubling. When we design an external resonator for an optimum mode matching with the fundamental wave, the thermal lens leads to a change in mode size and mode matching efficiency, which affects the effective operation of the external resonator. So it will be important to compare the SWC sensitivity with RC sensitivity caused by the thermal lens variation.

For a given resonator, the thermal focus length depends on the input power, and the large variation of the input power induces in large variation of the thermal focus length. A resonator is insensitive to the thermal lens variation, if its mode waist radius is insensitive to the change

of the thermal focus length. To have a low sensitivity with the input power variation, it is necessary to keep little spot size changes during the variation of the thermal focus length, and to mitigate the thermal effect as much as possible. Based on ABCD matrix, cavity parameter, and optimal cavity mode size, we can calculate the relationship between the thermal focus length and the waist size at the location of PPKTP crystal. The calculation results is shown in Fig. 4, which reveal that the mode waist radius is more sensitive to variation of thermal focus length for the SWC than that of for RC. If we follow the analysis results of section 3, considering the more sensitive of SWC overlap with severe thermal effect, the variation of the spot size for SWC is far more than that of for RC, when the variation of the input power is the same. The analysis results are shown in Fig. 5. The drastic variation of the waist radius changes the mode-matching efficiency from optimal to non-optimal value, which decreases the frequency-doubling conversion efficiency and power stability. The mode-matching efficiency to the cavity TEM<sub>00</sub> mode can be written as [25]

$$\kappa_{00} = \frac{16\Pi_{\alpha=x,y} \left\{ \int_0^l \frac{1}{W_{\alpha}^2(z) + W_{\alpha,e}^2(z)} dz \right\}^2}{\Pi_{\alpha} \left\{ \int_0^l \frac{1}{W_{\alpha}^2(z)} dz \right\} \left\{ \int_0^l \frac{1}{W_{\alpha,e}^2(z)} dz \right\}} \quad (6)$$

with Gaussian beam field, the  $W_{\alpha}(z)$  can be expressed to

$$W_{\alpha}^2(z) = W_{\alpha 0}^2 \left\{ 1 + \left( \frac{z - z_{\alpha}}{z_{\alpha 0}} \right)^2 \right\} \quad (7)$$

$$z_{\alpha 0} = \pi W_{\alpha 0}^2 / \lambda \quad (8)$$

where  $W_{\alpha}(z)$  and  $W_{\alpha 0}$  is the beam radius at  $1/e$  of the amplitude and the beam radius of the incident beam at the waist position  $z = z_{\alpha}$ , respectively;  $W_{\alpha,e}(z)$  and  $W_{\alpha,e 0}$  are that of the cavity eigenmodes.

In order to quantize the influence of the thermal lens on mode-matching efficiency [25], we analyze and obtain the relationship between mode-matching efficiency and the input power for the two cavity configurations, which is shown in Fig. 6. For the input power range from 0 to 1 W, the mode-matching efficiency decreases from 98% to 97.1% for the RC, to 91.7% for SWC. So the RC is more popular than SWC at higher power region.

## 5. Comparison of maximum output power

We performed the measurement of output power of second-harmonic wave with the two configurations described in Fig. 1. These experimental and theoretical results are summarized in Fig. 7. The discrete point is the measured experimental data for SWC and RC. Real lines are calculated theoretically. In the case of SWC, experiment result follows well with the theoretical calculated values for  $P_{in} < 150$  mW. After this value we see a deviation which becomes more marked as the pump power increasing. In the case of RC, the measured result has a deviation with the theoretical expectations when the output power is more than 88 mW at the input power of approximately 255 mW. The phenomenon can be explained by thermal gradient inside the crystal induced from the absorption. In the process of theoretical analysis, we omit the influence of temperature gradient on the mode-matching efficiency, phase-matching, thermal conductivity, thermo-optical coefficient, refractive index etc, which are considered as constant. In actual, all these parameters described above depend on the crystal temperature. The mode-matching efficiency reduces, and the phase-matching deviates from the optimal value, with the increase of temperature, which decrease the actual output power. From Ref. [26], the influence

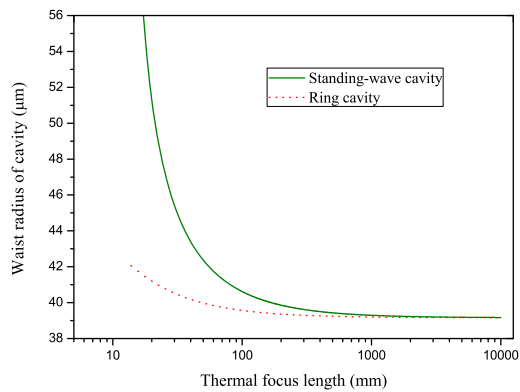


Fig. 4. Waist radius of the cavities at the location of the PPKTP crystal versus the thermal focus length.

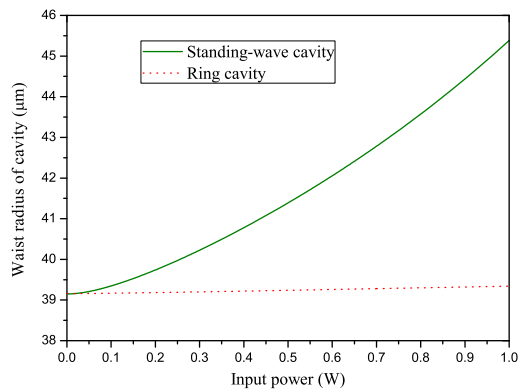


Fig. 5. Waist radius of the cavities at the location of the PPKTP crystal versus the input power.

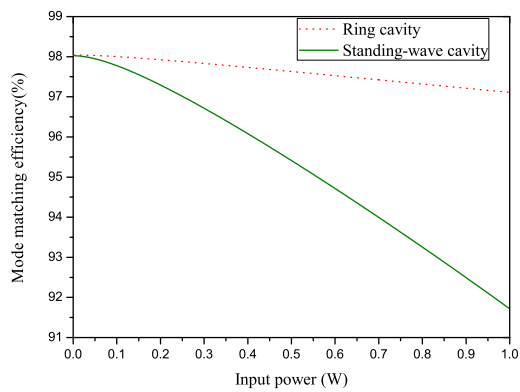


Fig. 6. Mode-matching efficiency between the input beam and external frequency-doubling cavity versus the input power.

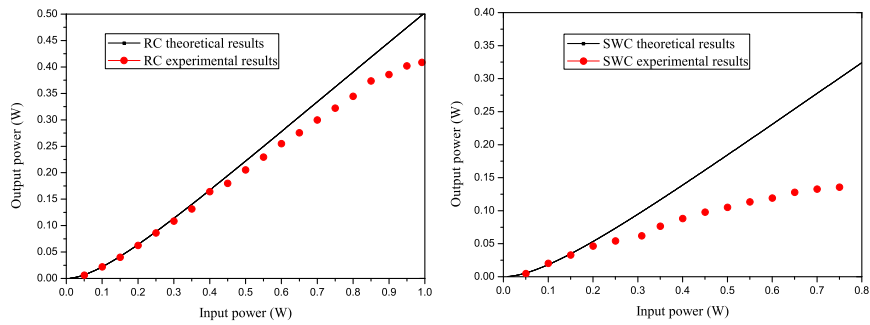


Fig. 7. Power of second harmonic wave versus the input power of the fundamental wave.

of the thermo-optical coefficient and refractive index can be omitted, the thermal conductivity is inverse proportional to the crystal temperature, which aggravate further the thermal effect. In addition, the heating does also result in an asymmetry of the resonant signal, thus bring about the deterioration of the error signal which will make it hard to the cavity locking at the top of the resonant signal peaks, and it decreases the output power of second harmonic further [27]. Comparing with RC, the SWC has a severer thermal effect, the deviation between theoretical and experimental results is larger [9]. For the SWC, with a mode-matching power of 784 mW, we get a maximum output power of 138 mW, corresponding to a conversion efficiency of 17.6%. Increasing further the input power, the output power decreases. For the RC, the maximum output power can be up to 408 mW, corresponding to a conversion efficiency of 41.9%, and the original mode-matching efficiency of 98%. Considering the final mode-matching efficiency of 93.4% (SWC) and 97.1% (RC), the two cavities's conversion efficiency are 18.8% (SWC) and 42.4% (RC), respectively. We did also measure the beam quality factor for the generated second harmonic out of the RC, by means of beam quality analyzer. We find the beam quality factor is 1.43 for horizontal direction, and 1.1 for vertical direction as shown in Fig. 8, which is suitable for the OPO pumping.

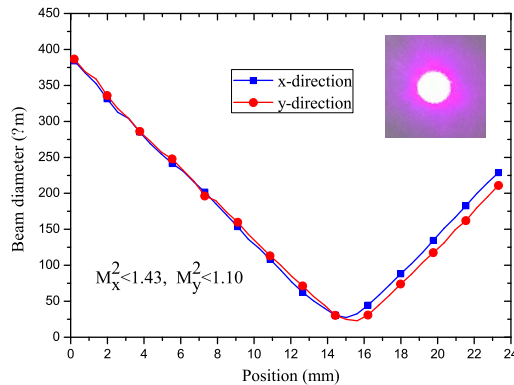


Fig. 8. Beam quality factor of the output beam.

## 6. Conclusion

We have theoretically and experimentally compared performance of linear standing-wave cavity and ring cavity for external cavity frequency doubling at the wavelength from 795 nm to 397.5 nm. The two cavity structure show obvious differences of the thermal effect in nonlinear crystal, cavity sensitivity, and maximum output power for same waist radius, linear loss and crystal length. In the case of SWC, due to double-pass beam propagation in the PPKTP crystal, its thermal effect is more severe than that in RC. Induced from the severe thermal effect, for the same variation of input power, the variation of thermal focus length located in the SWC is shorter than that of in RC. The SWC sensitivity is influenced by both the severe thermal effect and the characteristics of the cavity itself. In the RC, we obtain maximum output power of 408 mW, which is far higher than that of in SWC (only 138 mW). The phenomenon is explained as non-optimal phase-matching induced from the temperature gradient, non-optimal mode-matching induced from the thermal lens, and non-optimal resonant locking induced from the thermal effect meanwhile induced bistability. In the SWC, the power fluctuation is still a bit larger than that of in RC, which may be due either to cavity sensitivity or to fluctuation of the relative phase between forward- and backward directions of temperature change.

By using RC as the external resonator, we obtain maximal output power of 408 mW at 397.5 nm, with a beam quality factor of less than 1.43. The laser beam with good beam quality and enough output power can meet the requirements for pumping an OPO, which will promote the improvement of squeezed vacuum source at 795 nm resonant on Rubidium D1 line. We believe the output power can increase further with the enlargement of waist radius, which can meet the requirement for pumping more OPO and obtaining entanglement beams.

## Acknowledgements

This research is supported in part by the National Natural Science Foundation of China (Grant No. 61227015), in part by the Program for Outstanding Innovative Teams of Higher Learning Institutions of Shanxi, and in part by the Natural Science Foundation of Shanxi Province, China (Grant No. 2015021022).